Three-dimensional structure of the ribosomal translocase: elongation factor G from *Thermus thermophilus*

A.Ævarsson, E.Brazhnikov[1], M.Garber[1], J.Zheltonosova[1], Yu.Chirgadze[1], S.Al-Karadaghi, L.A.Svensson and A.Liljas[2]

Department of Molecular Biophysics, University of Lund, PO Box 124, S-221 00 Lund, Sweden and [1]Institute of Protein Research, Russian Academy of Sciences, 142292 Pushchino, Moscow Region, Russia
[2]Corresponding author

Communicated by A.S.Spirin

The crystal structure of *Thermus thermophilus* elongation factor G without guanine nucleotide was determined to 2.85 Å. This GTPase has five domains with overall dimensions of 50 × 60 × 118 Å. The GTP binding domain has a core common to other GTPases with a unique subdomain which probably functions as an intrinsic nucleotide exchange factor. Domains I and II are homologous to elongation factor Tu and their arrangement, both with and without GDP, is more similar to elongation factor Tu in complex with a GTP analogue than with GDP. Domains III and V show structural similarities to ribosomal proteins. Domain IV protrudes from the main body of the protein and has an extraordinary topology with a left-handed crossover connection between two parallel β-strands.
Key words: GTPase/GTP binding/guanine nucleotide exchange/protein topology/translocation

Introduction

Elongation factor G (EF-G, translocase) catalyses the translocation step of translation. This involves a conformational transition of the ribosome from the pre- to the post-translocational state with a movement of the mRNA and associated tRNAs, relative to the ribosome, placing the next codon of the mRNA in position to be translated in the next round of the elongation cycle (Kaziro, 1978; Spirin, 1985; Liljas, 1990; Nierhaus *et al.*, 1992).

EF-G belongs to the family of GTPases which are molecular switches able to alter between 'ON' and 'OFF' states: the active GTP conformation and the inactive GDP conformation, respectively (Bourne *et al.*, 1991). Among the subfamilies are the small GTPases like the Ras proteins including p21^{ras}, the heterotrimeric signal-transducing G proteins and the translation factors including EF-G (called EF-2 in eukaryotes and archaea), elongation factor Tu (EF-Tu; EF-1α in eukaryotes and archaea), initiation factor 2 (IF-2) and release factor 3 (RF-3) (Bourne *et al.*, 1990). They all share a common structural motif involved in the binding of guanine nucleotides and hydrolysis of GTP (Dever *et al.*, 1987). The general scheme of their functional cycle involves interactions with several components: (i) with the effector to which the ON signal is transmitted; (ii) with a GTPase activating protein (GAP); (iii) with a

guanine nucleotide exchange factor (GEF) to catalyse the exchange of GDP for GTP. For EF-G, no GEF exists and the effector and the GAP are parts of the ribosome (Bourne *et al.*, 1991).

EF-G catalyses the translocation upon binding of the EF-G−GTP complex to the ribosome, which in turn induces the GTPase activity of EF-G. The factor dissociates from the ribosome after GTP hydrolysis, GDP is released and the functional cycle is completed upon reactivation of the empty factor by binding of GTP (Liljas, 1991).

The binding site on the ribosome overlaps with the binding sites for EF-Tu, IF-2 and release factors 1 and 2 (Liljas, 1990). A number of ribosomal proteins have been cross-linked to EF-G, but the actual cross-linked residues have not been identified (Traut *et al.*, 1986). As shown by chemical footprinting, both EF-G and EF-Tu interact with the universally conserved α-sarcin loop of the 23S rRNA, whereas EF-G, but not EF-Tu, protects bases in the region around position 1070 to which EF-G has also been cross-linked (Sköld, 1983; Moazed *et al.*, 1988).

The crystal structures of three GTPases, p21^{ras} (Pai *et al.*, 1989; Milburn *et al.*, 1990), EF-Tu (Kjeldgaard and Nyborg, 1992) and the α subunit of transducin (Noel *et al.*, 1993), are already known. The single-domain structure of p21^{ras} is very similar to the N-terminal domain of EF-Tu, which contains two additional domains (Kjeldgaard and Nyborg, 1992). A similar domain also exists in EF-G, but this structural similarity accounts only for ~200 of a total of 691 residues in *Thermus thermophilus* EF-G (Yakhnin *et al.*, 1989).

We have determined the crystal structure of *T.thermophilus* EF-G, without bound nucleotide, at 2.85 Å resolution. The structure of EF-G with bound GDP is also determined (Czworkowski *et al.*, 1994) and is very similar. The protein is highly elongated and composed of five domains. Two domains are related to ribosomal proteins and RNA binding proteins, and two domains and their spatial relation are similar to the structure of EF-Tu with a bound GTP analogue (Berchtold *et al.*, 1993; Kjeldgaard *et al.*, 1993).

Results

Four of the five domains in EF-G (Figure 1A) are clustered together, whereas the fifth domain protrudes from the rest, making the molecule very extended and flat, the dimensions being 118 × 60 × 50 Å. The N-terminal domain, the G domain, is the nucleotide binding domain. The other domains are numbered consecutively along the sequence (II−V). Figure 1B shows an overview of the domain topology and a designation of the secondary structure elements. Strands are denoted by figures and helices by capital letters. Domains are denoted by a subscript.

The G domain shows great structural similarity to p21^{ras} and the G domain of EF-Tu, but it is substantially enlarged. The core of the G domain, with the consensus GTPase fold, is of the α/β structural class with a six-stranded mostly parallel β-sheet surrounded by five helices (Figure 1B). An insert of ~90 residues (residues 158–253), between helix D_G and strand 6_G, is called the G' subdomain. It begins as an extension of the sheet which continues into a β-meander of two β-hairpins making a four-stranded antiparallel sheet. This is followed by three helices before the polypeptide chain returns to the core domain.

The so-called 'effector' region in the G domain is disordered and not visible in our maps (residues 38–68). This may reflect the functional flexibility of this region, which is possibly involved in interactions with the ribosome and undergoes conformational changes upon GTP hydrolysis (Peter et al., 1990b).

Domain II is an all-β domain built up of 13 strands. The two first strands make a separate β-hairpin, whereas the others constitute a twisted β-barrel or a β-sandwich structure. Two strands (9_2 and 10_2) extend from the barrel towards the G domain and come in close proximity to strand 2_G and the invisible effector region.

Domains III, IV and V all contain four-stranded β-sheets with two helices on one side of the sheet, and belong to a subgroup of the α + β class called α–β sandwiches (Orengo and Thornton, 1993). Domain IV contains an additional β-sheet and a helix.

Domain III is disordered in the crystals and gives rather poor electron density. Thus, the model for this domain is not reliable and is incomplete. The probable connectivity of the secondary elements (1_3-A_3-2_3-3_3-B_3-4_3) is the same as for domain V (Figure 1B). The four strands and the two helices are antiparallel, and there is an internal 2-fold pseudosymmetry in the structure relating two topologically identical split βαβ motifs of two non-adjacent strands with a connecting helix (Orengo and Thornton, 1993).

Domain IV adds a bit of peculiarity to EF-G. It is protruding from the rest of the molecule and has an extraordinary topology. The main sheet is not anti-parallel, as expected for this type of structure (Orengo and Thornton, 1993). The parallel strands 4_4 and 7_4 and the connecting region, helix A_4 and the very short strands 5_4 and 6_4, make an exceptional left-handed 'βαβ' motif instead of the normal right-handed motif (Richardson, 1985). The small strands 5_4 and 6_4, the two strands connecting domain IV with domains III and V, and the C-terminal tail make a mixed five-stranded β-sheet with a helix at the very C-terminal end. This region of domain IV can be considered as an interdomain region and contains residues which are well conserved.

Domain V has the same topology as described for domain III and is of similar size. Domains II, III and V all make non-covalent contacts with a rather limited region of the G domain, mainly helices B_G and C_G.

Discussion

G domain and domain II
Both the core of the G domain and domain II are homologous to EF-Tu. Thus, ~40% of the structure of EF-G shows structural similarity to ~75% of EF-Tu

(Figures 1B and 2A). Domain III in EF-Tu has no homologous counterpart in EF-G, but occupies roughly the same space as domain V. A sequence alignment aided by the structural comparison of domain II in EF-Tu and EF-G shows that a similar domain probably also exists in IF-2, translation factor SELB (Forchhammer et al., 1989) and RF-3.

The structural conservation of the G domain and domain II implies that these domains together form a common structural unit possibly responsible for a similar ribosome interaction for all these different factors. A Gly to Val mutation (Gly280 in Salmonella typhimurium EF-Tu) in domain II renders the factor impaired in ribosome binding, whereas it seems functional in other respects (Tubulekas and Hughes, 1993). A Gly residue is also found at the corresponding position in EF-G (Gly379 in T.thermophilus) and probably also in IF-2 (Gly629 in Escherichia coli), translation factor SELB (Gly243 in E.coli) and RF-3 (Gly362 in E.coli).

The unusual fold of domain IV
Domain IV (Figure 3) has unexpected connectivity. The left-handed connection between strands 4_4 and 7_4 violates the empirical rule of the right-handedness of cross-over connections between parallel β-strands (Richardson, 1985). To our knowledge, there are only two other cases of a left-handed cross-over connection. One is in subtilisin, where the connecting helix contains the histidine residue of the catalytic triad (Wright et al., 1969). The second case is in the class 1 human leukocyte antigen (HLA), where the connecting helix forms a part of the antigen binding site and a region recognized by the T-cell receptor (Bjorkman et al., 1987). These exceptions to the right-handed connectivity suggest that part of the observed left-handed motif in EF-G may also be functionally important .

EF-2 is the specific target of diphtheria toxin which inactivates the factor by ADP-ribosylation of a certain post-translationally modified histidine residue (Ward, 1987). A reversible ADP-ribosylation of the same residue by a cellular mechanism may be important for the regulation of the activity of EF-2 in eukaryotic cells (Fendrick et al., 1992). Taking into account a slight ambiguity in the sequence alignment (Kohno et al., 1986; Cammarano et al., 1992), the corresponding residue is either located in the 7_4/B_4 loop or in the beginning of helix B_4 in EF-G (residues 576–583). This region is at the far end of domain IV and close to the left-handed cross-over connection (see Figure 3). Assuming similar overall structures of EF-G and EF-2, it is interesting to note that the binding of GTP to the G domain, at the other end of the molecule, inhibits the ADP-ribosylation by the diphtheria toxin (Sperti et al., 1971). The ADP-ribosylated EF-2 is impaired in ribosomal binding (Nygård and Nilsson, 1985) and the target residue has been claimed to be essential for the translocase activity of the factor (Omura et al., 1989).

Is EF-G related to ribosomal proteins?
The RNA binding proteins, like the small nuclear ribonucleoprotein U1A (Nagai et al., 1990; Hoffman et al., 1991) and several ribosomal proteins, have related folds (Lindahl et al., 1994). Domains III and V of EF-G have the same fold and there is a striking similarity between ribosomal protein S6 (Lindahl et al., 1994) and domain
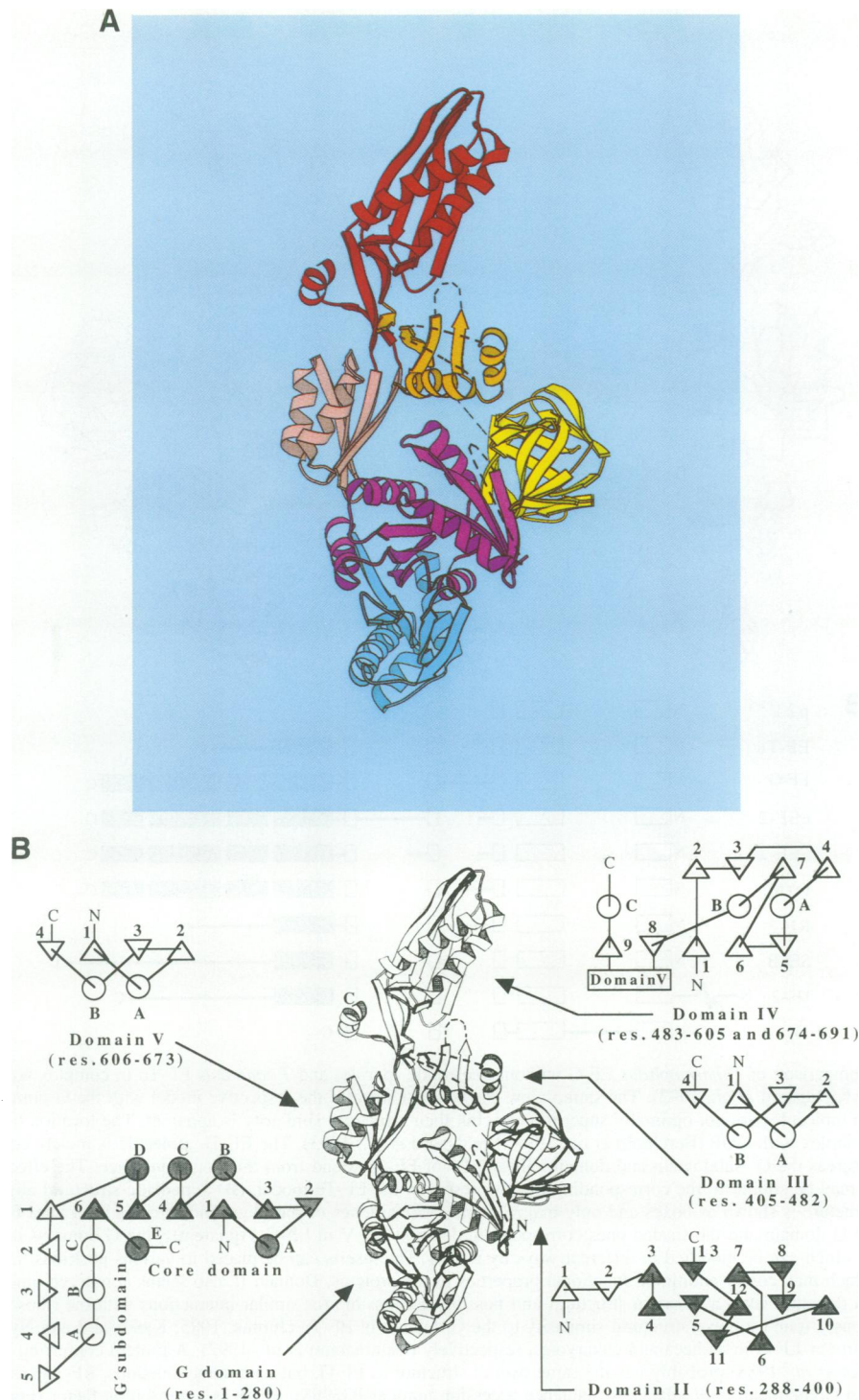
Fig. 1. (**A**) Schematic drawing of the structure of *T.thermophilus* EF-G in the absence of a guanine nucleotide. The different domains are coloured differently. The G domain consists of two different subdomains shown in different colours: violet for the core domain and blue for the G′ subdomain. Domain II is shown in yellow, III in orange, IV in red and V in pink. The crystallographic model contains ~90% of the residues, the rest being poorly or not visible in the electron density maps, most notably in domain III. The missing regions are indicated by dashed lines. The drawing was generated with the program MOLSCRIPT (Kraulis, 1991). (**B**) An overview of the domain topology and designation of secondary structure elements within each of the five domains. β-Strands are shown as triangles and helices as circles in the wiring diagrams. β-Strands are named by figures, helices are named by capital letters. The naming of the different elements is in keeping with the one used for the EF-G−GDP structure (Czworkowski *et al.*, 1994). The shaded elements in the G domain and domain II indicate the structural similarity to EF-Tu. The shaded core domain of the G domain corresponds to the consensus GTPase fold with the conserved sequence elements for nucleotide binding. The G′ subdomain is unique for EF-G. Owing to poor electron density, the structural model and topology of domain III are ambiguous, but it probably has the same topology as domain V.

V, with a r.m.s. deviation of 1.9 Å for 61 out of the 68 Cα atoms. The sequence identity between EF-G domain V and S6 from *T.thermophilus* is 18% (27% sequence similarity, including conservative substitutions). There are only five residues strictly conserved among EF-G/EF-2 sequences (Cammarano *et al.*, 1992) of domain V and
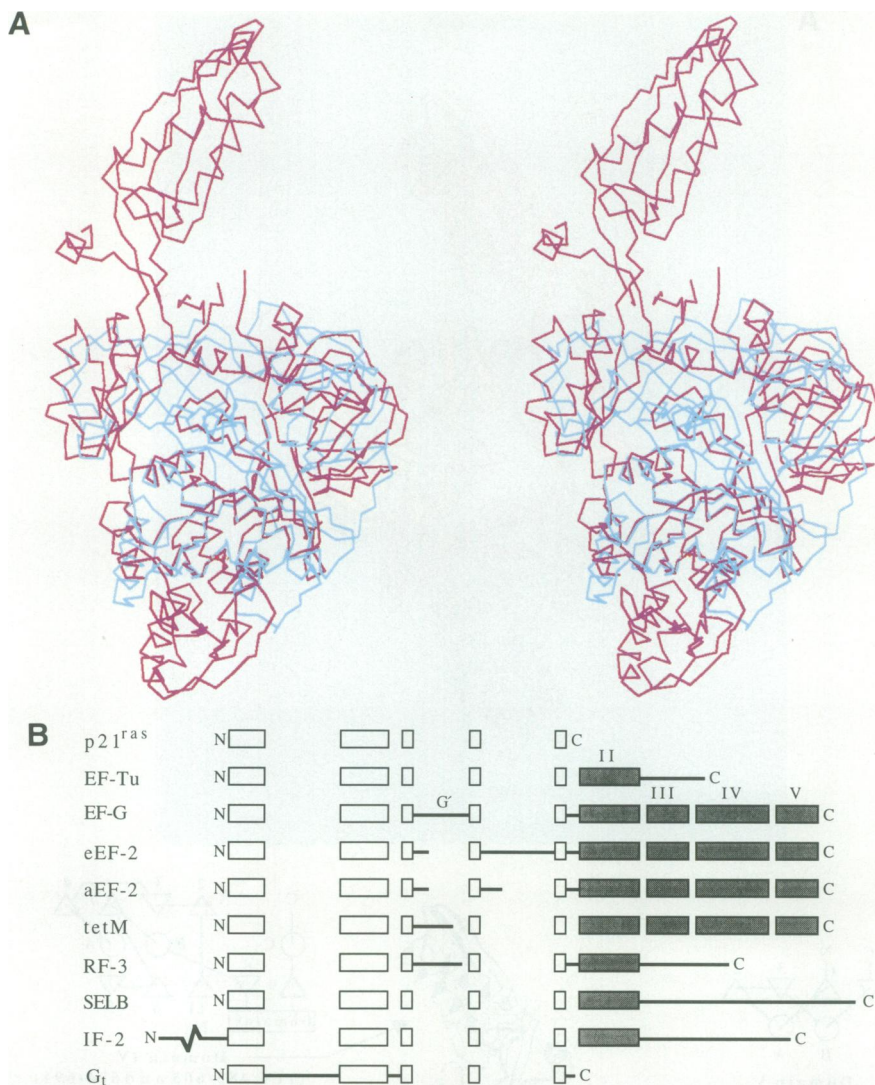
Fig. 2. (A) Structural comparison of *T.thermophilus* EF-G without nucleotide (purple) and *T.aquaticus* EF-Tu in complex with GTP analogue (blue) (Berchtold *et al.*, 1993; Kjeldgaard *et al.*, 1993). The stereo view shows a Cα trace of the respective model with the G domains superimposed. This way, domain IIs in both molecules are not optimally superimposed, but their structural similarity is apparent. The location of domain II is very different in EF-Tu in complex with GDP (Berchtold *et al.*, 1993; Kjeldgaard *et al.*, 1993). The EF-Tu molecule is mostly contained within the boundaries of EF-G, whereas the G′ subdomain and domains III and IV of EF-G extend from this common space. The effector region is missing in the EF-G model, but it may be similar to the corresponding region present in the EF-Tu model. **(B)** Schematic structural alignment of different GTPases. Conserved structure is shown as boxes and only major inserts (~20 residues or more) are indicated as bold lines between boxes. The white boxes correspond to the G domain and the shaded ones correspond to domains II−V in EF-G. Apparently, the G domains in GTPases have a common core structure which can be modified in different ways by inserts. The inserts can be placed in various positions, in some cases constituting separate subdomains which may confer additional functional properties to the proteins. Domain II also seems conserved among translation factors and together with the G domain makes a common structural unit possibly responsible for similar interactions with the ribosome. p21^{ras} is an oncogene protein previously found to have structural similarity to the G domain in EF-Tu (Jurnak, 1985; Kjeldgaard and Nyborg, 1992). aEF-2 and eEF-2 are the counterparts of EF-G in archaea and eukaryotes, respectively (Cammarano *et al.*, 1992). A protein conferring tetracycline resistance (tetM) (Sanchez-Pescador *et al.*, 1988) probably has the same overall structure as EF-G, but with some deletions. RF-3 is release factor 3 from *E.coli* (Mikuni *et al.* and Grentzmann *et al.*: database sequence accession number P33998). SELB is a translation factor (Forchhammer *et al.*, 1989). IF-2 is eubacterial initiation factor 2 (Gualerzi *et al.*, 1991). G$_t$ is the α subunit of transducin (Noel *et al.*, 1993).

two of those (Pro648 and Arg660) are also found in the two S6 sequences available. The similarity of domains III and V with ribosomal proteins may suggest that these domains are involved in interactions with RNA.

In U1A, the exposed face of the β-sheet is interacting with the RNA through exposed basic and aromatic residues, and similar interactions with rRNA have been suggested for S6 (Lindahl *et al.*, 1994). The face of the β-sheet in domain V of EF-G forms one side of a pronounced cleft formed between domains II and V with the switch II region of the G domain at the bottom. This cleft is lined by exposed aromatic and basic residues,

and is wide enough to accommodate a loop of double-stranded RNA.

Does EF-G have an internal GEF?

EF-G is exceptional among GTPases since it does not have a GEF, whereas EF-Tu requires elongation factor Ts (EF-Ts) as a specific GEF. It has been claimed that the relatively lower affinity of EF-G for GDP abolishes its need for a GEF (Bourne *et al.*, 1991). Domains II and III in EF-Tu interact with EF-Ts (Peter *et al.*, 1990a), but point mutations in the G domain show its importance for the binding of EF-Ts. This includes residues at the C-
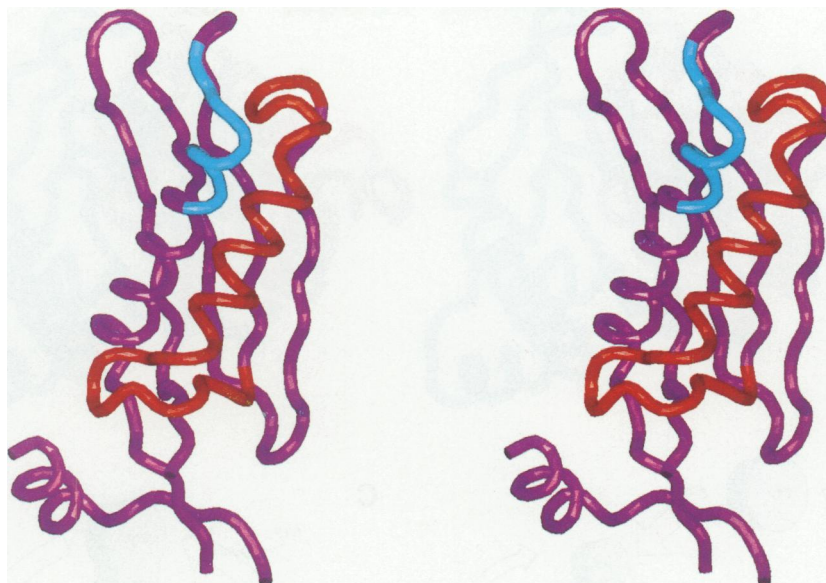
Fig. 3. A stereo illustration of domain IV. This domain has an exeptional folding with a very unusual left-handed cross-over connection shown in red between two parallel β-strands. This anomaly and the general topology is unexpected (Orengo and Thornton, 1993). Also shown in blue is the region corresponding to the site of ADP-ribosylation which inactivates EF-2 in eukaryotes and archaea. This region in EF-G corresponds to the site of ADP-ribosylation in EF-2 and may, together with some part of the adjacent structurally exceptional cross-over connection, form a functionally important region involved in ribosomal binding and/or more directly in the catalytic activity of the factor as translocase.

terminal part of the helix corresponding to E_G and in two loop regions (residues 136, 174, 176, 181, 196, 197 and 199 in *E.coli* EF-Tu) (Hwang *et al.*, 1992). The loop regions contain GTPase consensus elements with residues directly involved in the binding of guanine nucleotides. Similar regions of the α subunit of transducin and other GTPases have also been identified as sites of interaction with GEFs (Bourne *et al.*, 1991; Noel *et al.*, 1993).

The G' subdomain of EF-G makes extensive contacts with the core of the G domain corresponding to the binding sites for the respective GEF in the case of EF-Tu and transducin. Specifically, helix $C_{G'}$ interacts with a region close to the C-terminal end of helix E and the two β-hairpins of the G' subdomain are like two fingers with the fingertips touching loops $5_G/D_G$ and $6_G/E_G$ (Figure 4A). It is conceivable that the contacts between the G' sub-domain and the core of the G domain affect the binding of nucleotides. There are hydrogen bonds, either directly or through intervening residues, between residues in the G' subdomain and main chain atoms of residues involved in binding the nucleotide. This may imply that the G' subdomain functions as an intrinsic exchange factor modulating the binding of the guanine nucleotides and facilitating their exchange.

The G' subdomain of EF-G is found only among eubacteria, only a small insert is found at the same position in EF-2. However, the latter factors contain another insert in the G domain which probably has a similar location and function (Figure 2B). Sequence comparison (not shown) revealed the presence of a G' subdomain in RF-3 which shows good sequence similarity to EF-G for the β strands ($1_{G'}-5_{G'}$), but is slightly smaller than in EF-G.

The α subunit of transducin was found to contain a large insert, making a separate domain probably functioning as a GAP (Noel *et al.*, 1993). EF-G and transducin may thus be examples of exceptional GTPases not needing a conditional external stimulation of GDP dissociation and GTP hydrolysis, respectively, but which are engineered

by nature to provide the stimulation internally by additional domains (Figure 4B and C).

The nucleotide binding site and conformational changes

At least four distinct states can be distinguished during the functional cycle of the GTPases: from the inactive GDP state via the intermediate empty state to the active GTP state (Bourne *et al.*, 1991) and back to the GDP state via the GTPase state (Liljas, 1990). Previously, the crystal structures of three GTPases have been determined with a bound GTP analogue: p21^{ras} (Pai *et al.*, 1989; Brünger *et al.*, 1990; Milburn *et al.*, 1990), EF-Tu (Berchtold *et al.*, 1993; Kjeldgaard *et al.*, 1993) and the α subunit of transducin (Noel *et al.*, 1993). The structure of the inactive GDP form has also been published for both p21^{ras} (Milburn *et al.*, 1990) and EF-Tu (Kjeldgaard and Nyborg, 1992).

The present structure of EF-G is the first structural model of a member of this superfamily in the empty state. The structure of EF-G−GDP was solved at the same time in another laboratory (Czworkowski *et al.*, 1994) and is almost identical. For most of the residues directly involved in nucleotide binding, there is little deviation between the two states. The $1_G/A_G$ loop in the empty EF-G structure, containing the first consensus element, occupies the space otherwise occupied by the nucleotide and in particular the side chain of Ile21 is located in the same position as the phosphate moiety of the nucleotide (Figure 5A). The $2_G/B_G$ loop, including the Asp-X-X-Gly consensus element, and helix B_G form the 'switch II' region. Dramatic differences in this region are seen comparing the GDP and GTP forms of EF-Tu and p21^{ras}, most notably in the orientation of helix B_G (Milburn *et al.*, 1990; Schlichting *et al.*, 1990; Berchtold *et al.*, 1993; Kjeldgaard *et al.*, 1993). This region, in the present structure, is not very different from the GDP form of EF-G but differs very much from that of the EF-Tu−GDP structure (Kjeldgaard
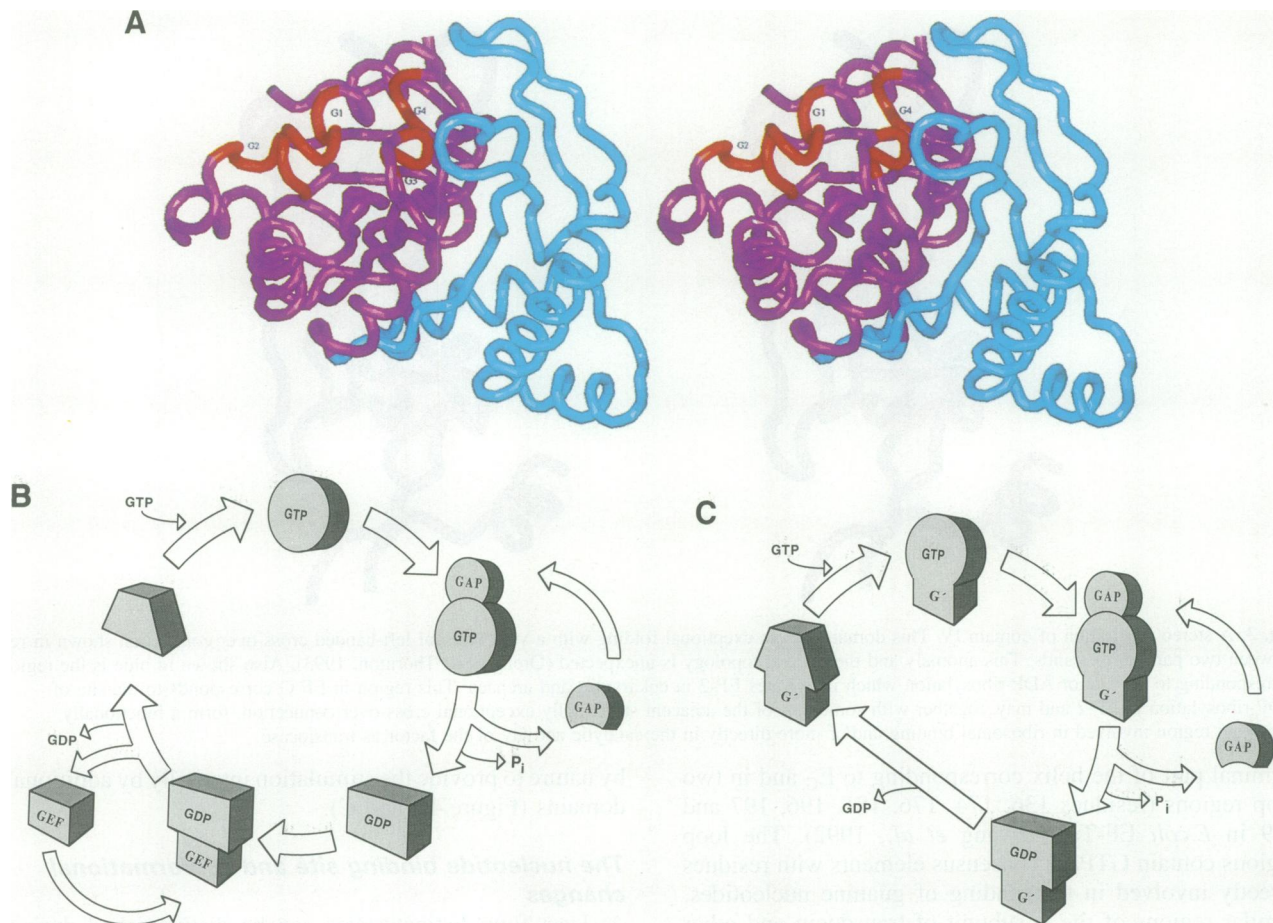
Fig. 4. (**A**) The G domain in EF-G shown in stereo with emphasis on the unique G′ subdomain shown in blue. The core of the G domain is shown in purple and corresponds to the consensus GTPase fold with conserved sequence elements shown in red and marked G1−G4. The 'fingers' of the G′ subdomain touch the loops with consensus elements G3 (Asn-Lys-x-Asp) and G4 (Ser-Ala-Leu/Lys). The specific contact regions of the core coincide with regions found to be important for interactions with GEFs in other GTPases (Bourne *et al.*, 1991; Hwang *et al.*, 1992; Noel *et al.*, 1993), suggesting that the G′ subdomain functions as GEF. (**B**) A general functional cycle for GTPases. The three general states are the active GTP state, the inactive GDP state and the empty state (Bourne *et al.*, 1991). The interaction with GAPs and/or GEFs induces additional states or conformations like the GTPase state (Liljas, 1990), leading to GTP hydrolysis upon binding to GAP. The active GTPase interacts with the effector which may be identical to the GAP or different. GEF may not dissociate until GTP is bound (Boguski and McCormick, 1993), and more complicated interactions between GTPase and GEF may exist (Kaziro *et al.*, 1991). (**C**) The functional cycle for EF-G. This cycle deviates from the general cycle by the absence of a GEF to facilitate the exchange of nucleotides. The G′ subdomain may function as intrinsic GEF, making EF-G able to take a 'shortcut' in the functional cycle. Similarly, transducin can go directly between the GTP state and the GDP state of the cycle since it has a large insert in the G domain (see Figure 2B), making a separate domain probably functioning as GAP (Noel *et al.*, 1993).

and Nyborg, 1992). On the other hand, the orientation of helix B$_G$ resembles that found in the GTP form of EF-Tu (Berchtold *et al.*, 1993; Kjeldgaard *et al.*, 1993).

The relative location of the G domain and domain II, in both the present structure and the GDP form, is similar to the one found in the GTP form, but not to the GDP form of EF-Tu. This implies that the same gross rearrangement of the domains upon GTP hydrolysis observed in EF-Tu (Berchtold *et al.*, 1993; Kjeldgaard *et al.*, 1993) does not occur in EF-G. However, EF-Tu and EF-G function in a reciprocal way: the active states of the factors catalyse the opposite directions of the transition of the ribosome between pre- and post-translocational states (Nierhaus *et al.*, 1992). This may be reflected in concerted conformational changes of the ribosome and the factors where the inactive conformation of one factor resembles the active conformation of the other.

The conformational change in EF-G upon GTP hydrolysis can be local, but greater changes in the overall structure cannot be excluded. As seen in Figure 5B, the switch II region is situated at the 'heart' of the molecule,

surrounded by three domains apart from the G domain, as well as the potential RNA binding cavity. Conceivably, a change in the conformation of the molecular switch can be transmitted from the G domain to each one of domains II, III or V and trigger a larger overall change, e.g. by domain rearrangements. Interestingly, the region of domain III in closest contact with the switch II region contains the only stretch of the sequence beyond the G domain with several consecutive strictly conserved residues (Gly-X-Gly-Glu-Leu-His, residues 453–458) which may play an important role in the conformational transitions.

The antibiotic fusidic acid (fus) specifically inhibits EF-G by forming a strong ribosome−EF-G−GDP−fus complex, where the factor is apparently locked in a certain conformation after GTP hydrolysis, possibly differing from any of the conformations of the free factor (Liljas, 1991). A clue to which parts of the molecule are involved in the binding of fusidic acid and/or affect conformational changes are the locations of mutations conferring fusidic acid resistance (Johanson and Hughes, 1994), which are confined to a central region of EF-G, including part of
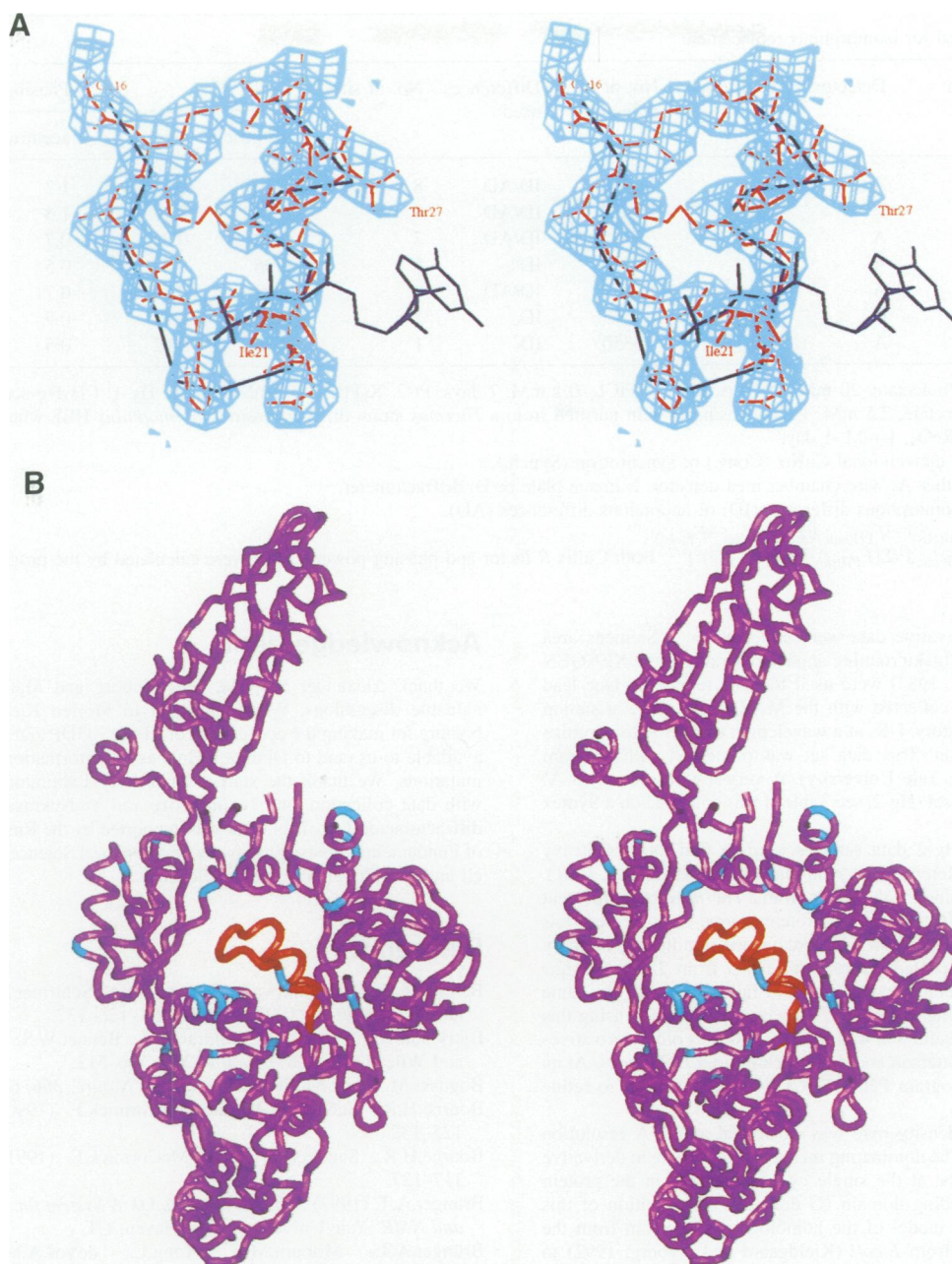
Fig. 5. (A) A part of the empty nucleotide site in *T.thermophilus* EF-G. Shown is the $3F_o-2F_c$ electron density map contoured at 1.0 σ. Superimposed on the density is the atomic model of residues 16–29 in red. Also shown in blue for comparison is the Cα trace of the corresponding residues (15–28) and the bound GTP analogue from the model of *T.aquaticus* EF-Tu in complex with GDPNP (Kjeldgaard *et al.*, 1993). This region has been called the phosphate binding loop and contains the consensus sequence element Gly/Ala-X-X-X-X-Gly-Lys-Thr/Ser (Ala19-His-Ile-Asp-Ala-Gly-Lys-Thr26 in *T.thermophilus* EF-G, called G1 in Figure 4A) with residues involved in binding the phosphates of the nucleotide. In the present empty state of EF-G, this loop has curled up and Ile21 moved into the space occupied by the phosphates when a nucleotide is bound. **(B)** A stereo view of the overall conformation of EF-G highlighting in red the conformational switch region (switch II) situated at the centre of the molecule. The structure of this switch region and the relative location of the G domain/domain II (Figure 2A) in the present empty structure and with bound GDP (this issue) resembles the structure found in the GTP form of EF-Tu (Berchtold *et al.*, 1993; Kjeldgaard *et al.*, 1993), but not the GDP form (Kjeldgaard and Nyborg, 1992), implying that different conformational changes are associated with GTP hydrolysis compared with EF-Tu. Conformational changes of this central interdomain switch region may be transmitted to any of the surrounding domains II, III or V, inducing greater conformational changes. Furthermore, switch II is still accessible from below and above for a possible interaction with the ribosome which functions both as the effector and the GTPase activator. Shown in blue are the locations of mutations found in mutants resistant to the antibiotic fusidic acid which locks EF-G on the ribosome, possibly by interfering with the conformational changes (Johanson and Hughes, 1994).

the interfaces between the G domain and domains III and V (Figure 5).

Materials and methods

Crystallization was done as previously described (Reshetnikova and Garber, 1983). The crystals were obtained in the absence of nucleotide and were subsequently cross-linked using glutaraldehyde. The crystals used for the structure determination contained EF-G purified from *T.thermophilus* HB8, except for one mercury derivative crystal (Hg-2, see Table I) which was obtained at a very early stage of the work with protein from a different *Thermus* strain. The crystals belong to space group $P2_12_12_1$ with one molecule in the asymmetric unit and cell dimensions of $75.59 \times 105.96 \times 116.43$ Å (Chirgadze *et al.*, 1983). Native crystals typically diffract to 2.8–3.0 Å at room temperature using a conventional X-ray source.

Table I. Derivatives used for isomorphous replacement

Derivative	Radiation source[a]	Detector[b]	Resolution (Å)	No. of reflections	Differences used[c]	No. of sites	Cullis R[d] acentric	centric	Phasing power[e] acentric	centric
Pb-1	Conv.	A	3.2	6930	ID/AD	8	0.70	0.66	1.7	1.2
Pb-2	Synch.	I	2.8	13 222	ID/AD	8	0.79	0.78	1.3	0.9
Pt-1	Conv.	A	3.2	7745	ID/AD	7	0.92	0.89	0.7	0.5
Pt-2	Conv.	A	3.2	9007	ID	5	0.96	0.93	0.5	0.3
Hg-1	Conv.	A	3.0	10 572	ID/AD	8	0.93	0.89	0.7	0.5
Hg-2	Conv.	D	8.0	575	ID	2	0.84	0.81	0.9	0.6
Re	Conv.	A	4.0	5350	ID	1	0.96	0.92	0.5	0.4

Pb-1 and Pb-2: $(CH_3)_3$Pb-acetate, 20 mM, 18 days. Pt-1: K_2PtCl_6, 0.1 mM, 7 days. Pt-2: K_2PtCl_6, 0.5 mM, 2 days. Hg-1: CH_3Hg-acetate, 2.5 mM, 3 days. Hg-2: CH_3Hg-acetate, 2.5 mM, 14 days using protein purified from a *Thermus* strain different from *T.thermophilus* HB8 which was otherwise used. Re: $NaReO_4$, 1 mM, 1 day.
[a]The radiation source is conventional $CuK\alpha$ (Conv.) or synchrotron (Synch.).
[b]The detector used is either A: wire chamber area detector, I: image plate or D: diffractometer.
[c]Differences used are isomorphous difference (ID) or anomalous differences (AD).
[d]Cullis R factor is $\Sigma|F_{PH(obs)}|-|F_{PH(calc)}|/\Sigma|F_{PH(obs)}-F_{P(obs)}|$.
[e]Phasing power is $[\Sigma|F_{H(calc)}|^2/\Sigma(F_{PH(obs)}|-|F_{PH(calc)}|)^2]^{1/2}$. Both Cullis R factor and phasing power values were calculated by the program MLPHARE (Otwinowski, 1991).

Native and most derivative data were collected on a Siemens area detector mounted on a Rigaku rotating anode. Programs in the XENGEN package (Howard *et al.*, 1987) were used for data reduction. One lead derivative data set was collected with the MAR image plate at station 9.5 of Daresbury Laboratory, UK, at a wavelength of 0.78 Å to optimize the anomalous dispersion. This data set was processed with program DENZO (Z.Otwinovski, Yale University). A very-low-resolution (8 Å) mercury derivative data set (Hg-2, see Table I) was collected on a Syntex P2₁ diffractometer.

The low-resolution Hg-2 data set was used to find the first heavy atom positions from difference Patterson maps (Chirgadze *et al.*, 1991). This derivative was obtained with protein from a *Thermus* strain different from *T.thermophilus* HB8, used as a protein source for other crystals used in this work, and was shown to contain one dominating mercury binding site. Despite repeated efforts with EF-G from *T.thermophilus* HB8 using the same mercury compound, we failed to obtain the same high occupancy of binding to this site. However, a derivative using this strain (Hg-1) was still useful and was solved as well as other derivatives using both difference Patterson and difference Fourier techniques. At an early stage, we used program PHARE (CCP4 program suite) to refine heavy atom parameters.

The initial electron density map was calculated at 3.5 Å resolution using four derivatives. The dominating mercury binding site in derivative Hg-2 was assumed to be at the single cysteine residue in the protein located in the GTP binding domain (G domain). The position of this site was used to fit the model of the homologous G domain from the EF-Tu−GDP structure from *E.coli* (Kjeldgaard and Nyborg, 1992) to this part of the map as an aid to building the model for this domain. All model building was done with the program O (Jones *et al.*, 1991). The phases were subsequently improved by using two additional derivative data sets. Native data were collected with higher resolution and better isomorphism to most of the derivatives, as judged using the program NORMAN (Howell, 1992). At this stage of the work, heavy atom parameters were refined and phases calculated with the program MLPHARE (Otwinowski, 1991) and solvent flattening, histogram matching and the use of Sayre's equation was applied with the program SQUASH (Zhang, 1993) to modify and extend the phases to 2.85 Å. Partial models, starting from a model of 30% of the structure, were refined and phases improved by phase recombination with the program SIGMAA (CCP4 program suite). Having built close to half of the structure, a big improvement in the quality of the map was made when the synchrotron derivative data set was included. The figure of merit was finally 0.50 for acentric reflections and 0.74 for centric reflections. The final model was refined with XPLOR (Brünger, 1992) using simulated annealing.

The native data are 84% complete to 2.85 Å. The current model of 626 residues (90%) has an R-factor of 23.4%, r.m.s. deviations of 0.021 Å in bond lengths and 4.42° in bond angles. Temperature factors were not refined and no solvent molecules were included in the model. The atomic coordinates will be deposited in the Brookhaven Protein Data Bank.

Acknowledgements

References

Berchtold,H., Reshetnikova,L., Reiser,C.O.A., Schirmer,N.K., Sprinzl,M. and Hilgenfeld,R. (1993) *Nature*, **365**, 126–132.
Bjorkman,P.J., Saper,M.A., Samraoui,B., Bennet,W.S., Strominger,J.L. and Wiley,D.C. (1987) *Nature*, **329**, 506–512.
Boguski,M.S. and McCormick,F. (1993) *Nature*, **366**, 643–654.
Bourne,H.R., Sanders,D.A. and McCormick,F. (1990) *Nature*, **348**, 125–132.
Bourne,H.R., Sanders,D.A. and McCormick,F. (1991) *Nature*, **349**, 117–127.
Brünger,A.T. (1992) *X-PLOR Version 3.0. A System for Crystallography and NMR.* Yale University, New Haven, CT.
Brünger,A.T., Milburn,M.V., Tong,L., deVos,A.M., Jancarik,J., Yamaizumi,Z., Nishimura,S., Ohtsuka,E. and Kim,S.-H. (1990) *Proc. Natl Acad. Sci. USA*, **87**, 4849–4853.
Cammarano,P., Palm,P., Creti,R., Ceccarelli,E., Sanangelantoni,A.M. and Tiboni,O. (1992) *J. Mol. Evol.*, **34**, 396–405.
Chirgadze,Yu.N., Nikonov,S.V., Brazhnikov,E.V., Garber,M.B. and Reshetnikova,L.S. (1983) *J. Mol. Biol.*, **168**, 449–450.
Chirgadze,Yu.N., Brazhnikov,E.V., Nikonov,S.V., Fomenkova,N.P., Garber,M.B., Urzhumtsev,A.G., Lunin,V.Yu., Chirgadze,N.Yu. and Nekrasov,Yu.V. (1991) *Dokl. Akad. Nauk SSSR* (English translation: *Dokl. Biochem. Proc. Acad. Sci. USSR*), **320**, 488–491.
Czworkowski,J., Wang,J., Steitz,T.A. and Moore,P.B. (1994) *EMBO J.*, **13**, 3661–3668.
Dever,T.E., Glynias,M.J. and Merrick,W.C. (1987) *Proc. Natl Acad. Sci. USA*, **84**, 1814–1818.
Fendrick,J.L., Iglewski,W.J., Moehring,J.M. and Moehring,T.J. (1992) *Eur. J. Biochem.*, **205**, 25–31.
Forchhammer,K., Leinfelder,W. and Böck,A. (1989) *Nature*, **342**, 453–456.
Gualerzi,C.O., Severini,M., Spurio,R., Lateana,A. and Pon,L. (1991) *J. Biol. Chem.*, **266**, 16356–16362.
Hoffman,D.W., Query,C., Golden,B.L., White,S.W. and Keene,J.D. (1991) *Proc. Natl Acad. Sci. USA*, **88**, 2495–2499.
Howard,A.J., Gilliland,G.L., Finzel,B.C., Poulos,T.L., Ohlendorf,D.H. and Salamme,F.R. (1987) *J. Appl. Crystallogr.*, **20**, 383–387.

Howell,P.L. (1992) *J. Appl. Crystallogr.*, **25**, 81–86.

Hwang,Y.W., Carter,M. and Miller,D.L. (1992) *J. Biol. Chem.*, **267**, 22198–22205.

Johanson,U. and Hughes,D. (1994) *Gene*, **143**, 55–59.

Jones,T.A., Zou,J.-Y., Cowan,S.W. and Kjeldgaard,M. (1991) *Acta Crystallogr. A*, **47**, 110–119.

Jurnak,F. (1985) *Science*, **230**, 32–36.

Kaziro,Y. (1978) *Biochim. Biophys. Acta*, **505**, 95–127.

Kaziro,Y., Itoh,H., Kozasa,T., Nakafuku,M. and Satoh,T. (1991) *Annu. Rev. Biochem.*, **60**, 349–400.

Kjeldgaard,M. and Nyborg,J. (1992) *J. Mol. Biol.*, **223**, 721–742.

Kjeldgaard,M., Nissen,P., Thirup,S. and Nyborg,J. (1993) *Structure*, **1**, 35–50.

Kohno,K., Uchida,T., Ohkubo,H., Nakanishi,S., Nakanishi,T., Fukui,T., Ohtsuka,E., Ikehara,M. and Okada,Y. (1986) *Proc. Natl Acad. Sci. USA*, **83**, 4978–4982.

Kraulis,P.J. (1991) *J. Appl. Crystallogr.*, **24**, 946–950.

Liljas,A. (1990) In Hill,W.E., Dahlberg,A., Garrett,R.A., Moore,P.B., Schlessinger,D. and Warner,J.R. (eds), *The Ribosome: Structure, Function and Evolution*. American Society of Microbiology, Washington, DC, pp. 309–317.

Liljas,A. (1991) *Int. Rev. Cytol.*, **124**, 103–135.

Lindahl,M., Svensson,L.A., Liljas,A., Sedelnikova,S.E., Eliseikina,I.A., Fomenkova,N.P., Nevskaya,N., Nikonov,S.V., Garber,M.B., Muranova,T.A., Rykonova,A.I. and Amons,R. (1994) *EMBO J.*, **13**, 1249–1254.

Milburn,M.V., Tong,L., deVos,A.M., Brünger,A., Yamaizumi,Z., Nishimura,S. and Kim,S.-H. (1990) *Science*, **247**, 939–945.

Moazed,D., Robertson,J.M. and Noller,H.F. (1988) *Nature*, **334**, 362–364.

Nagai,K., Oubridge,C., Jessen,T.H., Li,J. and Evans,P.R. (1990) *Nature*, **348**, 515–520.

Nierhaus,K.H., Schillingbartetzko,S. and Twardowski,T. (1992) *Biochimie*, 74, 403–410.

Noel,J.P., Hamm,H.E. and Sigler,P.B. (1993) *Nature*, **366**, 654–662.

Nygård,O. and Nilsson,L. (1985) *Biochim. Biophys. Acta*, **824**, 152–162.

Omura,F., Kohno,K. and Uchida,T. (1989) *Eur. J. Biochem.*, **180**, 1–8.

Orengo,C.A. and Thornton,J.M. (1993) *Structure*, **1**, 105–120.

Otwinowski,Z. (1991) In Wolf,W., Evans,P.R. and Leslie,A.G.W. (eds), *Isomorphous Replacement and Anomalous Scattering*. Science and Engineering Research Council, Warrington, WA4 4AD, UK, pp. 80–86.

Pai,E.F., Kabsch,W., Krengel,U., Holmes,K.C., John,J. and Wittinghofer,A. (1989) *Nature*, **341**, 209–214.

Peter,M.E., Reiser,C.O.A., Schirmer,N.K., Kiefhaber,T., Ott,G., Grillenbeck,W. and Sprinzl,M. (1990a) *Nucleic Acids Res.*, **18**, 6889–6893.

Peter,M.E., Schirmer,N.K., Reiser,C.O.A. and Sprinzl,M. (1990b) *Biochemistry*, **29**, 2876–2884.

Reshetnikova,L.S. and Garber,M.B. (1983) *FEBS Lett.*, **154**, 149–150.

Richardson,J.S. (1985) *Methods Enzymol.*, **115**, 341–358.

Sanchez-Pescador,R., Brown,J.T., Roberts,M. and Urdea,M. (1988) *Nucleic Acids Res.*, **16**, 1218.

Schlichting,I., Almo,S.C., Rapp,G., Wilson,K., Petratos,K., Lentfer,A., Wittinghofer,A., Kabsch,W., Pai,E.F., Petsko,G.A. and Goody,R.S. (1990) *Nature*, **345**, 309–315.

SERC (1979) *CCP4. Collaborative Computing Project No. 4, a Suite Of Programs for Protein Crystallography*. Daresbury Laboratory, Warrington WA4 4AD, UK.

Sköld,S.E. (1983) *Nucleic Acids Res.*, **11**, 4923–4932.

Sperti,S., Montanaro,L. and Mattioli,A. (1971) *Chem.-Biol. Interactions*, **3**, 141–148.

Spirin,A.S. (1985) *Prog. Nucleic Acids Res. Mol. Biol.*, **32**, 75–113.

Traut,R.R., Tewari,D.S., Sommer,A., Gavino,G.R., Olson,H.M. and Glitz,D.G. (1986) In Hardesty,B. and Kramer,G. (eds), *Structure, Function, and Genetics of Ribosomes*. Springer-Verlag, New York, pp. 286–308.

Tubulekas,I. and Hughes,D. (1993) *J. Bacteriol.*, **175**, 240–250.

Ward,W.H.J. (1987) *Trends Biochem. Sci.*, **12**, 28–31.

Wright,C.S., Alden,R.A. and Kraut,J. (1969) *Nature*, **221**, 235–242.

Yakhnin,A.V., Vorozheykina,D.P. and Matvienko,N.I. (1989) *Nucleic Acids Res.*, **17**, 8863.

Zhang,K.Y.J. (1993) *Acta Crystallogr. D*, **1**, 213–222.